High expression of eIF4E regulates immune cell infiltration and leads to poor prognosis in breast cancer

Fan Li
Tianjin Medical University
Huizhi Sun
Tianjin Medical University
Yue Li
Tianjin Medical University
Xiaoyu Bai
Tianjin Medical University
Xueyi Dong
Tianjin Medical University
Nan Zhao
Tianjin Medical University
Jie Meng
Tianjin Medical University
Baocun Sun
Tianjin Medical University
Danfang Zhang (zhangdf@tmu.edu.cn)
Tianjin Medical University

Research Article

Keywords: Eukaryotic translation initiation factor 4E (eIF4E), breast cancer, prognosis, immune infiltration, cytokines

Posted Date: March 15th, 2021

DOI: https://doi.org/10.21203/rs.3.rs-168436/v2

Abstract

Background

The expression and activation of Eukaryotic translation initiation factor 4E (eIF4E) is related to tumor transformation and genesis, but the functional role and the mechanism whereby it drives immune infiltration in breast cancer remain uncertain.

Methods

Multiple databases were used for assessing the expression and clinic-pathological features of eIF4E, after which ImmuCellAI and TIMER database were used to explore the relationship between eIF4E and immune infiltration and clinicopathological information were collected from clinical cases of breast cancer. Finally, the genes co-expressed with eIF4E were identified by LinkedOmics. These genes were analyzed protein interaction network and TF-miRNA interaction network by Networkanalyst, and enriched by GO and KEGG. The key genes of immune markers were functionally annotated.

Results

High expression of eIF4E was associated with poor overall survival (OS) and relapse-free survival (RFS) in breast cancer samples from multiple databases. It is notable that the expression of eIF4E is positively correlated with the infiltration of $CD8^+$T cells, macrophages, neutrophils and dendritic cells. The expression of eIF4E is closely related to many immune markers in breast cancer. Immunohistochemical analysis showed that the patients with high expression of eIF4E related macrophage marker ($CD68^+$) and M2 type marker ($CD163^+$) in tumor stroma(TS) were significantly correlated with poor prognosis ($P < 0.05$). High infiltration density of $CD163^+$ had significant difference in TNM staging compared with those with low($P < 0.05$).Functional analysis of co-expressed genes showed that they were involved in the biological process of human immune response. GO analysis showed that co-expressed immune marker genes were involved in human immune response, adaptive immune response, macrophage activation, extracellular structure organization and regulation of DNA metabolism process. KEGG enrichment showed that it was involved in inflammatory bowel disease, cell adhesion molecule pathway, JAK-STAT signal pathway, T cell receptor signal pathway and so on.

Conclusions

These results suggest that high expression of eIF4E regulates immune cell infiltration, especially promotes macrophage M2 polarization by JAK/STAT6 and PI3K/AKT pathway, which is associated with poor prognosis of breast cancer patients. It is a valuable prognostic biomarker for breast cancer patients, and may be a potential therapeutic target in the future.

1. Background

Breast cancer is the most common malignancy in women worldwide and is curable in 70–80% of patients with early, non-metastatic disease. Advanced breast cancer with distal organ metastases is considered incurable with currently available treatments (1).In 2019, about 316,700 new BC cases will be diagnosed in women in the United States, an annual increase of nearly 0.3%. Data from China show that the incidence of BC will be also increasing every year (272,400 cases in 2015 and 367,900 cases in 2018) (2).Breast cancer is considered as composed of at least four different clinically relevant molecular subtypes: luminal A, luminal B, Her2-Enriched, and basal-like type(3).

EIF4E is one of the essential constituent factors of protein initiation factor complex (eukaryotic translation initiation factor4, eIF4F) in eukaryotic protein translation initiation stage. mRNA caps containing 7-methylguanosine are recognized and bound in the early stages of protein synthesis, and ribosome binding is promoted by inducing the release of the secondary structure of mRNA. As a proto-oncogene, its expression and activation are related to tumor transformation and genesis. Selective translation regulation of mRNA transcripts usually occurs at the beginning, which can be achieved by specific RNA binding proteins, microRNA and regulating the activity of 5'cap binding eIF4E(4, 5). Previous studies have shown that patients with high expression of eIF4E are more likely to relapse and have higher mortality than minimal expression of eIF4E in patients with TNBC (6).

Here, we used Oncomine, PrognoScan and Kaplan-Meier to evaluate the relationship between eIF4E and prognosis. We further considered the relationship between eIF4E and tumor immune cell infiltration using tumor immunoassay resources (ImmuCellAI and TIMER). Our results provide new insights into the functional role of eIF4E in breast cancer. Thus highlighting the potential mechanism of eIF4E affecting the interaction between immune cells and tumors.

2. Methods

2.1 Clinical samples

Fifty breast cancer specimens were obtained from the General Hospital of Tianjin Medical University (Tianjin, China). These specimens were collected from patients between 1998 and 2006. The diagnosis of breast cancer in these samples was verified by two or more pathologists. Detailed pathological and clinical data were collected for all samples. The use of these tissue samples was approved by the Ethics Committee of Tianjin Medical University.

2.2 Immunohistochemistry

The tissues were deparaffinized in xylene and rehydrated in graded alcohols. First, 3% H_2O_2 was used to block endogenous peroxidase, followed by antigen retrieval. Tissue sections were blocked in 10% goat serum (Zhongshan Chemical Co., Beijing, China) and incubated consecutively with primary antibodies and a secondary antibody. Mouse anti human $CD68^+$ monoclonal antibody (zm-0060) and mouse anti

human $CD163^+$ monoclonal antibody (zm-0428) are all products of Beijing Zhongshan Jinqiao biotechnology company. Known positive tissue sections are used as positive control, and PBS is used as negative control instead of primary antibody. On the immunohistochemical section, $CD68^+$ and $CD163^+$ were expressed in the cytoplasm of macrophages, and the positive macrophages were yellow brown or brown granules. First, the whole section was observed under a low power (100 times) optical microscope. Five non overlapping high power fields (400 times) in the stroma were selected to count the positive cells. The average value of the count was taken as the final result of the expression of the sample. According to the staining results, the best cut-off value was selected as the decision point of high and low expression. The number of $CD68^+$ macrophages in tumor nests(TN)less than 14.4 was defined as low expression group and more than 14.4 as high expression group; the number of $CD68^+$ macrophages in tumor stroma(TS) less than 18.6 was defined as low expression group and more than 18.6 as high expression group; the number of $CD163^+$ macrophages in TN less than 19.58 was defined as low expression group, The number of $CD163^+$ macrophages in TS less than 27.6 was defined as low expression group, and the number of $CD163^+$ macrophages more than 27.6 was defined as high expression group.

2.3 Oncomine database analysis

The Oncomine database compiled 86,733 samples and 715 gene expression data sets into a single comprehensive database designed to facilitate data mining efforts(7). We therefore used this database to assess the association between eIF4E expression and prognostic outcome in various cancer types (https://www.oncom ine.org/resource/login.html).

2.4 PrognoScan database analysis

The PrognoScan database is designed to facilitate meta-analyses of gene prognostic value by comparing the relationship between gene expression and relevant outcome including overall survival (OS) in a wide range of published cancer microarray data sets(8). We therefore used this database to assess the relationship between eIF4E expression and patient outcome (http://www.abren.net/PrognoScan/).

2.5 Kaplan-Meier plotter analysis

The Kaplan-Meier plotter offers a means of readily exploring the impact of a wide array of genes on patient survival in 21 different types of cancer, with large sample sizes for the breast (n = 6,234), ovarian (n = 2,190), lung (n = 3,452) and gastric (n = 1,440) cancer cohorts(9).We therefore used this database to explore the association between eIF4E expression and outcome in patients with gastric, breast, ovarian and lung cancer (http://kmplot.com/analysis/).

2.6 TIMER database analysis

TIMER (https://cistrome.shinyapps.io/timer/) is a database designed for the analysis of immune cell infiltrates in multiple cancers. This database employs pathological examination-validated statistical methodology in order to estimate tumor immune infiltration by neutrophils, macrophages, dendritic cells,

B cells and $CD4^+$/$CD8^+$T cells(10). We initially employed this database to assess differences in eIF4E expression levels in particular tumor types using the TIMER database, and we then explored the association between this eIF4E expression and the degree of infiltration by particular immune cell subsets. Then Kaplan-Meier curve analysis and multi-factor COX proportional hazard model were carried out to explore the effect of immune cell infiltration on the survival rate of breast cancer patients. Finally, the relationship between the expression of eIF4E and the expression of specific immune infiltrating cell subsets was evaluated.

2.7 GEPIA database analysis

GEPIA (http://gepia.cancer-pku.cn/index.html) is an online database that can be used for standardized TCGA and GTEx dataset analysis of tumor samples and control samples (11). GEPIA database was used to evaluate the relationship between the expression of eIF4E and the prognosis of patients, as well as the subgroup analysis of clinical pathological features.

2.8 ImmuCellAI database analysis

The ImmuCellAI tool can accurately predict the abundance of 24 kinds of immune cells in the sample, including 18 kinds of T cell subtypes(12), based on the expression data of RNA-Seq or microarray. We used the Gene Expression Omnibus (GEO; http://www.ncbi.nlm.nih.gov/geo/) data set GSE109169 to analyze the difference of gene expression between breast cancer tissues and normal tissues adjacent to the cancer, and estimated the immunized cell infiltration abundance by using ImmuCellAI data bank (http://bioinfo.life.hust.edu.cn/web/ImmuCellAI/).

2.9 LinkedOmics database analysis

The LinkedOmics database (http://www.linkedomics.org/login.php) is a web-based platform for analyzing 32 TCGA cancer-associated multi-dimensional datasets(13). EIF4E co-expression was analyzed statistically using Pearson's correlation coefficient, presenting in volcano plots, heat maps, or scatter plots. The functional module of LinkedOmics analyzed gene ontological biological process (GO_BP), KEGG pathway, kinase target enrichment, miRNA target enrichment and transcription factor target enrichment by gene set enrichment analysis(GSEA).

2.10 Networkanalyst database analysis

Network interpreting gene expression was used by NetworkAnalyst 3.0 tool (https://www.network analyst.ca/)(14), which integrates cell-type or tissue specific protein-protein interaction(PPI) networks, gene regulatory networks, and gene co-expression networks.

2.11 Enrichment analysis of GO and KEGG pathways

The data base (DAVID v.6.8) and the data base(DAVID.ncifcrf.gov/) were used to identify the enrichment analysis (15). The biological process of GO and the enrichment analysis of KEGG pathway were carried

out on the key genes of co-expression and immune marker gene cross, and the visualization was made by Cytoscape v3.7.2 software(16) and R4.0.2 language. The *P* value adjusted by FDR was statistically significant.

2.12 Human protein Altas database

The expression of eIF4E and related immune markers in breast cancer was verified by HPA database (https://www.proteinatlas.org/). The protein expression in 44 major human tissues and some tumor tissues was expressed by the immunohistochemical method (17).

2.13 Statistical analysis

Statistical analyses were performed with SPSS 22.0 (SPSS Inc., Chicago, IL, USA). Values are expressed as the mean ± SD (standard deviation). The chi-squared test was used to compare categorical variables. Prognoscan, Kaplan-Meier plotter, TIMER and GEPIA databases were used for generating survival plots in respective analyses, with data including either HR and P-values or P-values derived from a log-rank test. Data from the Oncomine database are presented with information regarding ranking, fold-change and P-values. Pearson or Spearman's correlation analyses were used to gauge the degree of correlation between particular variables, with the following r values being used to judge the strength of correlation: 0.00–0.19 ‘very weak’,0.20–0.39 ‘weak’,0.40–0.59 ‘moderate’,0.60–0.79 ‘strong’,0.80–1.0 ‘very strong’. $P < 0.05$ was the significance threshold.

3. Result

3.1 Expression of eIF4E in different tumors and normal tissues

We first analyzed the expression of eIF4E in a variety of tumors and normal tissues using Oncomine database, and found that the expression of eIF4E in brain cancer, breast cancer, cervical cancer, colorectal cancer, gastric cancer, head and neck tumor, kidney cancer, lung cancer, lymphoma, ovarian cancer, pancreatic cancer, sarcoma and other tumors was higher than that in normal tissues ($P < 0.001$) (Fig. 1A). We further used the TIMER database to evaluate the differential expression of eIF4E in specific tumor types (Fig. 1B). The results showed that the expression of eIF4E in invasive breast carcinoma, endometrial carcinoma, cholangiocarcinoma, colonic adenocarcinoma, hepatocellular carcinoma, gastric adenocarcinoma, lung squamous cell carcinoma, lung adenocarcinoma and esophageal carcinoma was significantly higher than that in normal controls. The expression of eIF4E in thyroid carcinoma, renal papillary cell carcinoma and renal clear cell carcinoma was significantly lower than that in normal control groups. The expression in metastatic skin melanoma was higher than that in skin melanoma ($P < 0.05$).

Further subgroup analysis of multiple clinic-pathological features of TCGA-Breast invasive carcinoma samples in the UALCAN database consistently showed an increase in the transcriptional level of eIF4E. According to the analysis of sample type, age, subtype of breast cancer, disease stage, lymph node metastasis and TP53 mutation, the expression of eIF4E in breast cancer patients was significantly higher

than that in normal controls, and the expression of eIF4E in patients aged 61 to 80 was significantly higher than that in patients aged 41 to 60, with statistical difference ($P = 0.037399$). In all subtypes of breast cancer, the expression of eIF4E was significantly higher than that of normal subjects, and the expression of Luminal type was significantly higher than that of Triple negative type ($P < 0.01$), and the expression levels of stage1, stage2 and stage3 in different tumor stages were significantly higher than those in normal group. Lymph node metastasis showed that the expression level of N2 was the highest and significantly different from that of N0 ($P = 0.0127978$) and N3 ($P = 0.0169045$). TP53 mutation analysis showed that the expression level of TP53 non-mutated group was higher than that of the mutant group ($P = 0.024296$) (Fig. 2). Therefore, according to the expression differences of breast cancer subtypes, tumor stages and lymph node metastasis, the expression of eIF4E can be used as a potential diagnostic index in BRCA.

3.2 Relationship between eIF4E expression and prognosis of patients with different tumors

Next, we used the PrognoScan database to explore the relationship between the expression of eIF4E and the prognosis of tumor patients. We found that breast and colorectal cancers were significantly associated with the expression of eIF4E (Fig. 3A-B) (DSS: Disease Specific Survival; RFS: Relapse Free Survival).In addition, we used the Kaplan-Meier database to evaluate the relationship between the expression of eIF4E in a range of tumor types and prognosis. The results showed that the increased expression of eIF4E was significantly correlated with the poor prognosis of breast cancer (OS HR = 1.32, 95% CI = 1.02–1.71, $P = 0.037$; HR = 1.41, 95% CI = 1.27–1.857, $P = 5.3e\text{-}10$). The increased expression of eIF4E was also significantly associated with poor prognosis in ovarian cancer (OS HR = 1.1810 95%CI = 1.02–1.36, $P = 0.026$). However, in lung and gastric cancers, decreased expression of eIF4E was significantly associated with poor prognosis (lung cancer OS HR = 0.86, 95%CI = 0.76–0.98 $P = 0.019$; gastric cancer OS HR = 0.54, 95%CI = 0.44–0.65 $P = 1.1e\text{-}10$) (Fig. 3C-G). We further used GEPIA database to evaluate the relationship between the expression of eIF4E and the prognosis of patients, and analyzed 33 tumor types. It was found that the prognosis of high expression of eIF4E was poor in breast cancer, brain low-grade glioma, lung adenocarcinoma, cervical squamous cell carcinoma and adenocarcinoma, hepatocellular carcinoma and lung squamous cell carcinoma, while the low expression of eIF4E in renal clear cell carcinoma, hepatic clear cell carcinoma and colorectal cancer had poor prognosis(Supplement Fig. 1A-I).These results clearly showed that in many tumor types, the expression of eIF4E was significantly correlated with poor prognosis, and the high expression of eIF4E in different databases was significantly correlated with poor prognosis of breast cancer patients.

3.3 Relationship between eIF4E expression and infiltration of immune cells in breast cancer

Gene expression data set GSE109169, related to breast cancer was searched from the comprehensive gene expression database (GEO) to analyze the difference of gene expression between breast cancer and adjacent normal tissues (Supplementary table1).The abundance of immune cell infiltration was calculated by ImmuCellAI database. It was found that in 18 kinds of T cells and other 6 types of immune cells, the infiltration levels of macrophages, nTreg cells, Th1, B cells, $CD8^+$T cells and γδT cells in breast

cancer tissues were significantly higher than those in adjacent normal tissues. Infiltration levels of Th17 cells, Tfh, NKT cells, monocytes, neutrophils and $CD4^+$T cells in tumor tissues were lower than those in normal tissues (Fig. 4). This showed that there are a significant difference in immune cell infiltration between breast cancer patients and adjacent normal tissues, and different levels of immune cell infiltration have potential effects on the occurrence, development and survival of breast cancer patients.

Since we found that the expression of eIF4E was related to the poor prognosis of patients with breast cancer, we further drew a Kaplan-Meier map using the TIMER database to explore the relationship between immune cell infiltration and the expression of eIF4E to explore its potential mechanism in breast cancer. In breast cancer, eIF4E expression was significantly correlated with tumor purity (r = 0.134 P = 2.21e-05), $CD8^+$T cells(r = 0.268 P = 1.51e-17), macrophages (r = 0.237 P = 5.07e-14), neutrophils(r = 0.161 P = 6.14e-07) and dendritic cells (r = 0.067 P = 3.94e-02) (Fig. 5A).

In order to further study the relationship between immune cell infiltration and eIF4E expression in BRCA, we further used TIMER database to generate Kaplan-Meier map. We found that the infiltration of $CD8^+$T cells (P = 0.006), $CD4^+$T cells (P = 0.006), neutrophils (P = 0.007) and dendritic cells (P = 0.004) was significantly correlated with the prognosis of BRCA (Fig. 5B). In addition, the multivariate hazard model was used to evaluate the effect of eIF4E expression in the presence of different immune cell infiltration. The OS risk of eIF4E was 1.482 times higher (P < 0.05) (Fig. 5C). This suggested that eIF4E played an important role in regulating immune cell infiltration in breast cancer.

3.4 Evaluation of the correlation between eIF4E and the expression of immune markers

Next, we used TIMER databases to further explore the relationship between the expression of eIF4E and the level of immune cell infiltration in breast cancer. We evaluated the correlation between eIF4E expression and specific cell subsets, including $CD8^+$T cells, B cells, monocytes, TAMs, M1 and M2 macrophages, neutrophils, NK cells, DC, Th1 cells, Th2 cells, Tfh cells, Th17 cells, Treg cells and Exhaustion T cells. We adjusted these results according to the purity of the tumor. $CD8^+$T cells (CD8B), B cells (CD19, CD79A), monocyte markers (CD86), TAM markers (CCL2, CD68, IL10), M1 macrophage markers (COX2), M2 macrophage markers (CD163, VSIG4, MS4A4A), Neutrophils markers (CD11b), DC markers (HLA-DPB1, HLA-DRA, HLA-DPA1, BCDA-4), Th1 markers (STAT4, STAT1), Th2 markers (GATA3, STAT6), Tfh markers (BCL6, IL21), Th17 (STAT3), Treg markers (FOXP3, CCR8, STAT5B), Exhaustion T cell makers(PD-1, LAG3, TIM-3) were significantly correlated with eIF4E expression (Table 1).The expression of eIF4E in breast cancer was positively correlated with the expression of monocytes, TAM, M1 macrophages, M2 macrophages, Neutrophils, Th1, Th2, Tfh, Th17 and Treg markers, and negatively correlated with CD8 + T cells, B cells, dendritic cells and Exhaustion T cell markers. Figure 6A showed the scatter diagram of TAM, M2 macrophages, Th1, Th2, Th17, Treg and Exhaustion T cell markers.

Table 1
Correlation analysis between eIF4E and relate genes and markers of immune cells in TIMER.

Description	Gene makers	Breast cancer					
		None			Purity		
		Cor	P		partial.cor	partial.p	
CD8 + T cell	CD8A	-0.022	4.75×10 − 1		0.04686004	0.13985143	
	CD8B	-0.148	8.28×10 − 7	***	-0.10188943	0.00129684	*
T cell(general)	CD3D	-0.125	3.09×10 − 5	***	-0.06614794	0.03705509	*
	CD3E	-0.094	1.82×10 − 3	*	-0.02731704	0.38961155	
	CD2	-0.043	1.5×10 − 1		0.02692737	0.3964128	
B cell	CD19	-0.146	1.08×10 − 6	***	-0.09601416	0.00244306	*
	CD79A	-0.136	5.99×10 − 6	***	-0.0761307	0.01636396	*
Monocyte	CD86	0.096	1.47×10 − 3	*	0.15738691	6.1348E-07	***
	CD115(CSF1R)	0.001	9.73×10 − 1		0.0607296	0.05561681	
TAM	CCL2	0.002	9.39×10 − 1		0.06986978	0.02761177	*
	CD68	0.065	3.01×10 − 2		0.11656366	0.00023057	**
	IL10	0.153	3.38×10 − 7	***	0.21721067	4.4418E-12	***
M1 Macrophage	INOS(NOS2)	-0.024	4.34×10 − 1		-0.0130669	0.68072849	
	IRF5	0.016	5.91×10 − 1		0.03883945	0.22116287	
	COX2(PTGS2)	0.043	1.56×10 − 1		0.12822816	5.0261E-05	***

Cor, R value of Spearman's correlation; None, correlation without adjustment. Purity, correlation adjusted by purity. *P < .01; **P < .001;***P < .0001. Abbreviations: TAM, tumour-correlated macrophage; Tfh, follicular helper T cell; Th, T helper cell; Treg, regulatory T cell.

M2 Macrophage	CD163	0.152	4.1×10 − 7	***	0.20522705	6.4959E-11	***
	VSIG4	0.077	1.04×10 − 2		0.12544706	7.3161E-05	***
	MS4A4A	0.138	4.39×10 − 6	***	0.210251	2.1511E-11	***
Neutrophils	CD66b(CEACAM8)	-0.018	5.52×10 − 1		-0.01102645	0.72843176	
	CD11b(ITGAM)	0.041	1.76×10 − 1		0.08676308	0.00619708	*
	CCR7	-0.055	6.61×10 − 2		0.0154633	0.62630164	
Natural killer cell	KIR2DL1	-0.015	6.12×10 − 1		0.00357961	0.9102562	
	KIR2DL3	-0.008	7.97×10 − 1		0.0146039	0.64560698	
	KIR2DL4	-0.027	3.62×10 − 1		0.00685601	0.8290771	
	KIR3DL1	-0.04	1.82×10 − 1		-0.00907876	0.77497103	
	KIR3DL2	-0.051	9.37×10 − 2		-0.01393341	0.66083692	
	KIR3DL3	0.004	8.82×10 − 1		0.01473616	0.64262004	
	KIR2DS4	-0.028	3.57×10 − 1		0.01435843	0.65116604	
Dendritic cell	HLA-DPB1	-0.167	2.46×10 − 8	***	-0.11866431	0.000177	**
	HLA-DQB1	-0.113	1.75×10 − 4	**	-0.05129112	0.10606764	
	HLA-DRA	0.011	7.1×10 − 1		0.08384234	0.0081765	*
	HLA-DPA1	0.011	7.12×10 − 1		0.08372552	0.00826629	*
	BCDA-1(CD1C)	-0.083	5.95×10 − 3	*	-0.0070813	0.82355157	

Cor, R value of Spearman’s correlation; None, correlation without adjustment. Purity, correlation adjusted by purity. *P < .01; **P < .001;***P < .0001. Abbreviations: TAM, tumour-correlated macrophage; Tfh, follicular helper T cell; Th, T helper cell; Treg, regulatory T cell.

	BCDA-4(NRP1)	0.144	1.59×10−6	***	0.20736387	4.0736E-11	***
	CD11c(ITGAX)	-0.02	5.17×10−1		0.04743547	0.1350466	
Th1	T-bet(TBX21)	-0.096	1.45×10−3	*	-0.03946619	0.21379428	
	STAT4	0.024	4.34×10−1		0.10698215	0.00072919	**
	STAT1	0.275	1.62×10−20	***	0.29435209	2.558E-21	***
	IFN-γ(IFNG)	-0.033	2.75×10−1		0.0081502	0.79745787	
	TNF-α(TNF)	-0.068	2.51×10−2		-0.03221895	0.31021222	
Th2	GATA3	0.301	1.66×10−24	***	0.27086187	3.5639E-18	***
	STAT6	0.075	1.32×10−2		0.10105935	0.00142107	*
	STAT5A	0.001	9.78×10−1		0.04334184	0.17212936	
	IL13	-0.009	7.67×10−1		0.02091229	0.51017828	
Tfh	BCL6	0.062	4.01×10−2		0.10660096	0.00076196	**
	IL21	0.041	1.71×10−1		0.07605566	0.01647037	*
Th17	STAT3	0.304	5.92×10−25	***	0.31529031	2.2229E-24	***
	IL17A	-0.007	8.23×10−1		0.01164907	0.71375374	
Treg	FOXP3	0.006	8.53×10−1		0.07298812	0.02137316	*
	CCR8	0.217	3.19×10−13	***	0.27040878	4.0704E-18	***
	STAT5B	0.254	1.35×10−17	***	0.27303179	1.8794E-18	***

Cor, R value of Spearman’s correlation; None, correlation without adjustment. Purity, correlation adjusted by purity. *P < .01; **P < .001;***P < .0001. Abbreviations: TAM, tumour-correlated macrophage; Tfh, follicular helper T cell; Th, T helper cell; Treg, regulatory T cell.

	TGFβ(TGFB1)	-0.093	1.95×10 − 3	*	-0.0489941	0.12267125	
T cell exhaustion	PD-1(PDCD1)	-0.142	2.14×10 − 6	***	-0.09726802	0.00214011	*
	CTLA4	-0.037	2.15×10 − 1		0.02018994	0.52490196	
	LAG3	-0.14	3.09×10 − 6	***	-0.11585047	0.00025198	**
	TIM-3(HAVCR2)	0.133	9.24×10 − 6	***	0.18444976	4.6761E-09	***
	GZMB	-0.084	5.49×10 − 3	*	-0.03822992	0.22850157	

Cor, R value of Spearman's correlation; None, correlation without adjustment. Purity, correlation adjusted by purity. *P < .01; **P < .001;***P < .0001. Abbreviations: TAM, tumour-correlated macrophage; Tfh, follicular helper T cell; Th, T helper cell; Treg, regulatory T cell.

In addition, the protein expression level of eIF4E can be discovered by using clinical samples from HPA database. The immunohistochemical images showed that eIF4E shows moderate staining in breast cancer (Fig. 6B). At the same time, we verified the expression level of eIF4E significantly related immune cell markers in the same breast cancer patients, including TAM markers (IL10), M2 macrophage markers (CD163), Th1 (STAT1), Th2 (GATA3, STAT6), Th17 (STAT3) and Treg markers (STAT5B), in which GATA3, STAT3 and STAT5B were moderately stained and the others were weakly positive. The difference of expression of immune markers in tumor tissues of patients with breast cancer was further discussed.

In order to further verify the results of database analysis, we selected breast cancer samples for immunohistochemical staining of TAM macrophage marker (CD68) and M2 macrophage marker (CD163), and made clinicopathological analysis(Fig. 7). The results showed that the infiltration density of CD68 and CD163 in breast cancer nests was 15.2 ± 8.23 and 21.75 ± 9.18 per field, respectively; the infiltration density of CD68 and CD163 in breast cancer stroma was 20.59 ± 11.07 and 30.87 ± 12.95 per field, respectively. Pearson correlation test showed that the infiltration density of CD68 + and $CD163^+$ macrophages in TS was negatively correlated with survival time (r = -0.34, P = 0.016; r = -0.283, P = 0.047), but there was no significant difference in TN. Kaplan Meier survival curve analysis showed that the overall survival time (OS) of patients with high density of $CD68^+$ and $CD163^+$ in TS was significantly shorter than that of patients with low density (P < 0.05) (Fig. 7A-D). The analysis of $CD68^+$, $CD163^+$ macrophage infiltration density and clinicopathological parameters showed that the patients with high infiltration density of M2 macrophage marker $CD163^+$ in TS were significantly higher than those with low infiltration density in TNM stage III + IV (P < 0.05), but there was no significant difference in age, tumor diameter, lymph node metastasis and grade (P > 0.05) as shown in Table 2.

Table 2
The differences of postoperative clinical data between high and low expression of $CD68^+$ and $CD163^+$

Variables	$CD68^+$				$CD163^+$			
	Low	High	χ^2	P	Low	High	χ^2	P
Age			0.76	0.38			0.36	0.54
< 50	17	14			12	19		
≥ 50	8	11			9	10		
Tumor size			0.34	0.56			2.12	0.15
D□3	10	8			10	8		
D ≥ 3	15	17			11	21		
Lymphatic metastasis			0.86	0.35			0.04	0.85
No	16	19			15	20		
Yes	9	6			6	9		
Grade			2.60	0.11			0.09	0.76
□/□	21	16			16	21		
□	4	9			5	8		
TNM stage			1.44	0.23			4.02	0.045*
□+□	24	21			21	24		
□+□	1	4			0	5		
*Statistically significant p < 0.05								

3.5 Analysis of co-expression genes of eIF4E in breast cancer

In order to figure out the biological significance of eIF4E in BRCA, the functional module of LinkedOmics was used to check the co-expression pattern of eIF4E in the BRCA cohort. As showed in Fig. 8A, 5315 genes (dark red dots) were significantly positively correlated with eIF4E while 8395 genes (dark green dots) were negatively correlated. The heat map showed the first 50 important genes positively and negatively correlated with PRPF3 (Figure.8B and C), of which UBE2D3 ubiquitin binding enzyme had the highest positive correlation (r = 0.671112, *P* = 5.68E-144). The co-expressed genes were described in detail in the supplementary table2.

Gene ontology (GO) terminology annotations made through gene set enrichment analysis (GSEA) showed that genes co-expressed by eIF4E were mainly involved in chromosome segregation, RNA localization and DNA replication while extracellular structure organization, human immune response and protein localization to endoplasmic reticulum were inhibited(Fig. 8D, supplementary table3). KEGG enrichment showed that it was mainly concentrated in ubiquitin-mediated proteolysis, RNA transport, cell cycle and other signal pathways, while ribosome, glycosaminoglycan biosynthesis, cell adhesion molecules and other signal pathways were inhibited (Fig. 8E, supplementary table 4).

In addition, co-expressed network of protein-protein interactions by Differential Net was constructed based on breast-specific data collected from eIF4E database (Figure.9A, supplementary table5). The top three central genes were CUL3, heat shock protein 90αA1 (HSP90AA1) and YWHAZ. CUL3 is the core component of BCR (BTB-CUL3-RBX1) E3 ubiquitin protein ligase complex. The ubiquitin ligase complex mediates the ubiquitination of the target protein and subsequent proteasome degradation (18); the ubiquitin ligase complex BCR (KLHL25) participates in translation homeostasis by mediating ubiquitin and hypo-phosphorylated eIF4EBP1 (4E-BP1) degradation (19). Extracellular heat shock protein 90α (HSP90AA1) has been widely reported promoting tumor cell movement and tumor metastasis in many tumors. It has been observed that extracellular heat shock protein 90α can promote EMT and the migration of breast cancer cells in breast cancer (20). YWHAZ binds and stabilizes key proteins involved in signal transduction, cell proliferation and apoptosis (21). Studies have further shown that YWHAZ is involved in drug resistance in breast cancer (22).

Finally, the TF (transcription factor)-mi RNA regulatory interaction of eIF4E co-expressed genes was constructed based on RegNetwork database (Figure.9B, supplementary table6). The top three TF were upstream stimulating factor1 (USF1), CCCTC binding factor (CTCF) and transcription factor YY1. USF1 related studies have shown that USF1 can transcriptionally up-regulate the expression of FAK in lung cancer, thus activating the FAK signal pathway and promoting cell migration (23). USF1 is involved in the transcription of many proteins and plays an important role as a regulator in many diseases, including tumors(24).Studies have shown that CTCF expression is involved in tumorigenesis(25) and can be used as a transcription factor, to control gene expression by binding to the transcriptional initiation site(TSSs) of many genes(26).Some studies have shown that the binding and overexpression of transcription factor YY1 with BRCA1 promoter inhibits the proliferation and focus formation of nude mice cells and inhibits the growth of MDA-MB-231 tumor. In addition, tissue microarray detected that there was a positive correlation between the expression of YY1 and BRCA1 in human breast cancer (27, 28).

3.6 Cross analysis of eIF4E co-expression genes and immune marker genes

We showed that eIF4E co-expression gene GO analysis was involved in human immune-related biological processes, KEGG enrichment also showed that it was involved in the cell adhesion molecule pathway, which related to the expression of cytokines. In order to further explore the relationship between eIF4E co-expression genes and immune infiltration, we made a cross-analysis of 13710 co-expression genes and 30 immune marker genes significantly related to eIF4E. The results showed that there were 18

overlapping genes (Fig. 10A). The interaction of these key genes was analyzed by Cytoscape software and GO analysis. The results showed that the key genes were mainly involved in the human immune response, the adaptive immune response, macrophage activation, extracellular structure organization and regulation of DNA metabolic process (Fig. 10C). KEGG analysis showed that these key genes were mainly involved in inflammatory bowel disease (STAT4, HLA-DPB1, HLA-DRA, STAT6, FOXP3, HLA -DPA1), cell adhesion molecule pathways (CD8B, HLA-DPB1, PDCD1, HLA-DPA1), JAK-STAT signaling pathways (STAT4, STAT6), T cell receptor signaling pathway (PDCD1) (Fig. 10B). These results suggested that eIF4E co-expression genes were involved in the regulation of tumor immunity and provided strong evidence that eIF4E was an important regulator of immune infiltration in breast cancer.

4. Discussion

The activity of eIF4E is regulated at several levels, including PI3K (phosphatidylinositol 3-kinase) / AKT (also known as protein kinase B, PKB) / mTOR (mechanical / mammalian target of rapamycin) and RAS (rat sarcoma) / MAPK (mitogen activated protein kinase) / MNK (MAPK interacting kinase(29). EIF4E plays an important role in the whole process of tumor evolution. On one hand, eIF4E over expression changes cell morphology, enhances cell proliferation, and induces cell transformation, tumor formation and metastasis; on the other hand, eIF4E regulates the translation of tumor-related mRNA in many ways, including cell mitosis, activation of proto-oncogenes, angiogenesis, enhancement of autocrine, cell survival, invasion and communication with extracellular environment. Related studies have shown that eIF4E contains the original hypoxia response (HRE), in hypoxia microenvironment HIF1α up-regulates eIF4E, to promote selective mRNA cap-dependent translation (30).In order to better understand the potential function and regulatory network of eIF4E in breast cancer, we conducted a bioinformatics analysis of public data to guide future research on breast cancer.
Analysis of different tumor-related databases confirmed that the levels of eIF4E mRNA in breast cancer were significantly higher than those in normal breast tissues (Fig. 1). In addition, high expression of eIF4E was significantly associated with poor survival and disease-free status in multiple cohorts. Therefore, our results suggested that eIF4E was up-regulated in many breast cancer cases, which was worthy of further clinical verification as a potential diagnostic and prognostic marker.

In order to explore the signaling network controlling the abnormal expression of eIF4E, we draw eIF4E co-expression network. Our results indicate that eIF4E was involved in the biological functions of chromosome segregation, RNA localization and DNA replication, while extracellular structure organization, human immune response and protein localization to endoplasmic reticulum were inhibited. The main pathways involved include ubiquitin-mediated proteolysis, cell cycle, RNA transport, ribosome, Glycosaminoglycan biosynthesis and cell adhesion molecule pathway. These findings were related to the carcinogenic molecules pathway of breast cancer, which gave a reasonable explanation for the negative correlation between the expression of EIF4E and the 5-year survival rate of patients with breast cancer, and suggested that eIF4E was related to immune response, and gave clues to regulate tumor microenvironment and immune response.

We further found that the expression of eIF4E was related to the expression of several different markers of immune cell subsets in tumors, which highlighted the possible role of eIF4E in tumor immune interaction in breast cancer, making it a valuable biomarker worthy of further study. We found that the expression of eIF4E was positively correlated with the degree of $CD8^+$T and macrophage infiltration in breast cancer, and weakly positively correlated with the degree of DC and neutrophil infiltration (Fig. 5A). In addition, the correlation between the expression of eIF4E and some immunological marker genes strongly suggested that eIF4E can control the infiltration and interaction of immune cells in the tumor microenvironment in breast cancer. We observed a positive correlation between eIF4E and TAM, M2 macrophage markers (including CCL2, CD68, IL10, CD163, VSIG4 and MS4A4A) (Table 1), indicating that eIF4E has a role in regulating TAM polarization. The results of immunohistochemical analysis showed that there was significant difference in TNM staging between the high infiltration density group and the low infiltration density group in TS ($P < 0.05$), which indicated that TAM polarization and TS infiltration promoted the malignant progression of breast cancer,. Consistent studies have shown that TAM can secrete a variety of angiogenic factor, such as VEGF, MMP9, tumor necrosis factor (TNF), TGF-β, EGF, fibroblast growth factor (FGF) to promote angiogenesis(31, 32).TAM is transformed into M2 to enhance tumor angiogenesis in advanced tumors (33). In breast cancer, TAM can also secrete matrix metalloproteinase 9 (MMP9) and matrix metalloproteinase 2 (MMP2) to degrade the extracellular matrix, M2 can produce high level of MMP, promote extracellular matrix (ECM) degradation, and stimulate tumorigenesis, cancer cell invasion and metastasis by activating Epithelial-mesenchymal transition (EMT)(31, 34). Previous studies have demonstrated that IFN-γ can regulate the metabolism and translation of human macrophages by targeting kinases mTORC1 and MNK, both of which act on the selective regulators of translation initiation eIF4E (5). Because of the correlation between the expression of eIF4E and macrophage related genes, we inferred that the expression of eIF4E was involved in macrophage infiltration. We further found that eIF4E levels in breast cancer were associated with markers of Treg cell and Exhaustion T cell (FOXP3, CCR8, STAT5B, PD-1, LAG3 and TIM-3) (Table 1). Related studies have shown that Tim-3 promotes liver cancer through NF –κ B/IL- 6/STAT3 axis(35); FOXP3 is essential to maintain Treg inhibition function(36). This suggested that eIF4E might inhibit T-cell-mediated immunity by promoting Treg response. In addition, eIF4E expression was considered to be associated with the expression of multiple T cell subsets (Th1, Th2, Tfh, and Th17) in breast cancer. This might suggest the ability of eIF4E to regulate T cell response in breast cancer. As an immune marker of Th17, STAT3 expression was significantly positively correlated with eIF4E (Fig. 6). Related studies have shown that some signal molecules are involved in M2 polarization of macrophages, such as PI3K/ AKT-ERK signal, STAT3, HIF1α, STAT6 and so on. M2 macrophages promote the progression of breast cancer through ERK/STAT3 regulation (37). Consistent studies have shown that eIF4E was regulated by the PI3K/ AKT /mTOR pathway to promote the translation of cytokines (38).

The overlapping gene function and pathway enrichment of co-expressed genes and immune marker genes significantly related to eIF4E also showed that they were involved in tumor-related pathways such as cell adhesion molecule pathway, JAK-STAT signal pathway, immune-related biological processes such as adaptive immune response, macrophage activation, extracellular structure and regulation of DNA

metabolism. Taken together, these results highlighted the potential ability of eIF4E to regulate the recruitment and activation of immune cells in breast cancer.

Our results showed that the expression of eIF4E was positively correlated with CD68, CD163, STAT4 and STAT6, suggesting that eIF4E has a potential role in promoting M2 polarization of macrophages. Macrophage polarization is a complex process of multi factor interaction, which is regulated by a variety of intracellular signaling molecules and pathways, including JAK-STAT and PI3K/AKT signaling pathways. M2 macrophages play an important role in angiogenesis, secretion of anti-inflammatory factors, tissue repair and wound healing. Studies have shown that M2 macrophages can promote tumor progression (39). STAT6 is the main signal of IL-4-mediated signaling pathway, and JAK / STAT6 pathway is the main pathway from the cell membrane to the nucleus, which ultimately regulates the gene expression in the nucleus and mediates the differentiation and maturation of M2 cells(40).Th2 can activate macrophages by secreting IL-4 and / or IL-13 through signal transducers and activators of transcription 6 (STAT6) signal, which makes them have completely different characteristics from the classical activation(41, 42). At the same time, PI3K / AKT pathway regulates the survival, migration and proliferation of macrophages, but also coordinates the response of macrophages to different metabolic and inflammatory signals(43). PI3K activation has been reported as an essential step toward M2 activation of macrophages in response to surfactant protein A or IL-4. AKT activation is necessary for M2 activation, because AKT inhibition eliminates the up-regulation of M2 genes (44). EIF4E is downstream of PI3K / AKT pathway, which further suggests that eIF4E has potential promoting effect on M2 polarization of macrophages (Fig. 11).

Conclusions

In conclusion, high expression of eIF4E regulates immune cell infiltration, especially promotes macrophage M2 polarization by JAK / STAT6 and PI3K / AKT pathway, which is associated with poor prognosis of breast cancer patients. EIF4E is a valuable prognostic biomarker and may be used as a potential therapeutic target in the future. These findings need further research on breast cancer genomics and function.

Abbreviations

Eukaryotic translation initiation factor 4E (eIF4E)，relapse-free survival (RFS)，eukaryotic translation initiation factor4,，eIF4F，，overall survival (OS)，tumor stroma(TS)，tumor nests，TN，，heat shock protein 90αA1 (HSP90AA1)，Gene ontology (GO)，gene set enrichment analysis (GSEA)， transcription factor (TF)， upstream stimulating factor1 (USF1)，CCCTC binding factor (CTCF)，transcriptional initiation site(TSSs)， phosphatidylinositol 3-kinase (PI3K)， AKT (also known as protein kinase B, PKB) ， mechanical / mammalian target of rapamycin (mTOR) ， rat sarcoma (RAS)，mitogen activated protein kinase (MAPK)， MAPK interacting kinase (MNK)，original hypoxia response (HRE)，tumor necrosis factor (TNF)，fibroblast growth factor (FGF)，matrix metalloproteinase 9 (MMP9)，matrix metalloproteinase 2 (MMP2)，Epithelial-mesenchymal transition (EMT)，extracellular matrix (ECM)

Declarations

Ethics approval and consent to participate The experimental protocol was established, according to the ethical guidelines of the Helsinki Declaration and was approved by the Human Ethics Committee of Tianjin Medical University. Written informed consent was obtained from individual or guardian participants.

Consent for publication Not applicable

Availability of data and materials The GSE109169 datasets generated during and analyses during the current study are available in the GEO database(http://www.ncbi.nlm.nih.gov/geo/). Oncomine database analysis during the current study are available in https://www.oncom ine.org/resource/login.html.PrognoScan database analysis during the current study are available in http://www.abren.net/PrognoScan/. Kaplan-Meier plotter analysis during the current study are available in http://kmplot.com/analysis/. TIMER database analysis during the current study are available in https://cistrome.shinyapps.io/timer/. GEPIA database analysis during the current study are available in http://gepia.cancer-pku.cn/index.html. LinkedOmics database analysis during the current study are available in http://www.linkedomics.org/login.php. Networkanalyst database analysis during the current study are available in https://www.network analyst.ca/. Human protein Altas database analysis during the current study are available in https://www.proteinatlas.org/.

In addition,since pathological and clinical data involve patient privacy, if you want to obtain it or other information, please contact the corresponding author.

Competing interests The authors declare that they have no competing interests.

Funding:This research was funded by the project of National Nature Science Foundation of China (Nos. 81773076) and the project of Nature Science Foundation of Tianjin (No. 19JCYBJC25600).

Authors' contributions: Conceptualization, F.L. and D.Z.; methodology, F.L., Y.L. and H.S.; software, F.L., X.B and X.D.; validation, F.L., N.Z. and J.M.; formal analysis, F.L. and Y.L.; resources, B.S.; data curation, F.L.; writing—original draft preparation, F.L.; writing—review and editing, F.L. and D.Z.; visualization, F.L.; supervision, X.B., X.D. and N.Z; project administration, B.S. and D.Z; funding acquisition, D.Z. All authors have read and agreed to the published version of the manuscript.

Acknowledgements:This research was funded by the project of National Nature Science Foundation of China (Nos. 81773076) and the project of Nature Science Foundation of Tianjin (No. 19JCYBJC25600).

References

1. Harbeck N, Penault-Llorca F, Cortes J, Gnant M, Houssami N, Poortmans P, et al. Breast cancer. Nature reviews Disease primers. 2019;5(1):66.

2. DeSantis CE, Ma J, Gaudet MM, Newman LA, Miller KD, Goding Sauer A, et al. Breast cancer statistics, 2019. CA: a cancer journal for clinicians. 2019;69(6):438–51.
3. Harbeck N, Gnant M. Breast cancer. Lancet. 2017;389(10074):1134–50.
4. Piccirillo CA, Bjur E, Topisirovic I, Sonenberg N, Larsson O. Translational control of immune responses: from transcripts to translatomes. Nature immunology. 2014;15(6):503–11.
5. Su X, Yu Y, Zhong Y, Giannopoulou EG, Hu X, Liu H, et al. Interferon-gamma regulates cellular metabolism and mRNA translation to potentiate macrophage activation. Nature immunology. 2015;16(8):838–49.
6. Bhat M, Robichaud N, Hulea L, Sonenberg N, Pelletier J, Topisirovic I. Targeting the translation machinery in cancer. Nature reviews Drug discovery. 2015;14(4):261–78.
7. Rhodes DR, Kalyana-Sundaram S, Mahavisno V, Varambally R, Yu J, Briggs BB, et al. Oncomine 3.0: genes, pathways, and networks in a collection of 18,000 cancer gene expression profiles. Neoplasia. 2007;9(2):166–80.
8. Mizuno H, Kitada K, Nakai K, Sarai A. PrognoScan: a new database for meta-analysis of the prognostic value of genes. BMC medical genomics. 2009;2:18.
9. Lanczky A, Nagy A, Bottai G, Munkacsy G, Szabo A, Santarpia L, et al. miRpower: a web-tool to validate survival-associated miRNAs utilizing expression data from 2178 breast cancer patients. Breast cancer research and treatment. 2016;160(3):439–46.
10. Li T, Fan J, Wang B, Traugh N, Chen Q, Liu JS, et al. TIMER: A Web Server for Comprehensive Analysis of Tumor-Infiltrating Immune Cells. Cancer research. 2017;77(21):e108-e10.
11. Tang Z, Li C, Kang B, Gao G, Li C, Zhang Z. GEPIA: a web server for cancer and normal gene expression profiling and interactive analyses. Nucleic Acids Res. 2017;45(W1):W98-W102.
12. Miao YR, Zhang Q, Lei Q, Luo M, Xie GY, Wang H, et al. ImmuCellAI: A Unique Method for Comprehensive T-Cell Subsets Abundance Prediction and its Application in Cancer Immunotherapy. Advanced science. 2020;7(7):1902880.
13. Vasaikar S, Straub P, Wang J, Zhang B. LinkedOmics: Analyzing multi-omics data within and across 32 cancer types. Cancer research. 2019;79(13).
14. Zhou G, Soufan O, Ewald J, Hancock REW, Basu N, Xia J. NetworkAnalyst 3.0: a visual analytics platform for comprehensive gene expression profiling and meta-analysis. Nucleic Acids Res. 2019;47(W1):W234-W41.
15. Huang DW, Sherman BT, Lempicki RA. Systematic and integrative analysis of large gene lists using DAVID bioinformatics resources. Nature protocols. 2009;4(1):44–57.
16. Doncheva NT, Morris JH, Gorodkin J, Jensen LJ. Cytoscape StringApp: Network Analysis and Visualization of Proteomics Data. Journal of proteome research. 2019;18(2):623–32.
17. Uhlen M, Fagerberg L, Hallstrom BM, Lindskog C, Oksvold P, Mardinoglu A, et al. Proteomics. Tissue-based map of the human proteome. Science. 2015;347(6220):1260419.

18. Scott DC, Rhee DY, Duda DM, Kelsall IR, Olszewski JL, Paulo JA, et al. Two Distinct Types of E3 Ligases Work in Unison to Regulate Substrate Ubiquitylation. Cell. 2016;166(5):1198–214 e24.
19. Yanagiya A, Suyama E, Adachi H, Svitkin YV, Aza-Blanc P, Imataka H, et al. Translational homeostasis via the mRNA cap-binding protein, eIF4E. Molecular cell. 2012;46(6):847–58.
20. Tian Y, Wang C, Chen S, Liu J, Fu Y, Luo Y. Extracellular Hsp90alpha and clusterin synergistically promote breast cancer epithelial-to-mesenchymal transition and metastasis via LRP1. Journal of cell science. 2019;132(15).
21. Bergamaschi A, Katzenellenbogen BS. Tamoxifen downregulation of miR-451 increases 14-3-3zeta and promotes breast cancer cell survival and endocrine resistance. Oncogene. 2012;31(1):39–47.
22. Wang W, Zhang L, Wang Y, Ding Y, Chen T, Wang Y, et al. Involvement of miR-451 in resistance to paclitaxel by regulating YWHAZ in breast cancer. Cell death & disease. 2017;8(10):e3071.
23. Jiang W, Cai F, Xu H, Lu Y, Chen J, Liu J, et al. Extracellular signal regulated kinase 5 promotes cell migration, invasion and lung metastasis in a FAK-dependent manner. Protein & cell. 2020;11(11):825–45.
24. Sun Q, Li J, Li F, Li H, Bei S, Zhang X, et al. LncRNA LOXL1-AS1 facilitates the tumorigenesis and stemness of gastric carcinoma via regulation of miR-708-5p/USF1 pathway. Cell proliferation. 2019;52(6):e12687.
25. Debaugny RE, Skok JA. CTCF and CTCFL in cancer. Current opinion in genetics & development. 2020;61:44–52.
26. Nora EP, Goloborodko A, Valton AL, Gibcus JH, Uebersohn A, Abdennur N, et al. Targeted Degradation of CTCF Decouples Local Insulation of Chromosome Domains from Genomic Compartmentalization. Cell. 2017;169(5):930–44 e22.
27. Lee MH, Lahusen T, Wang RH, Xiao C, Xu X, Hwang YS, et al. Yin Yang 1 positively regulates BRCA1 and inhibits mammary cancer formation. Oncogene. 2012;31(1):116–27.
28. Khachigian LM. The Yin and Yang of YY1 in tumor growth and suppression. International journal of cancer. 2018;143(3):460–5.
29. Siddiqui N, Sonenberg N. Signalling to eIF4E in cancer. Biochemical Society transactions. 2015;43(5):763–72.
30. Yi T, Papadopoulos E, Hagner PR, Wagner G. Hypoxia-inducible factor-1alpha (HIF-1alpha) promotes cap-dependent translation of selective mRNAs through up-regulating initiation factor eIF4E1 in breast cancer cells under hypoxia conditions. The Journal of biological chemistry. 2013;288(26):18732–42.
31. Hingorani DV, Lippert CN, Crisp JL, Savariar EN, Hasselmann JPC, Kuo C, et al. Impact of MMP-2 and MMP-9 enzyme activity on wound healing, tumor growth and RACPP cleavage. Plos One. 2018;13(9):e0198464.
32. Li W, Liang RR, Zhou C, Wu MY, Lian L, Yuan GF, et al. The association between expressions of Ras and CD68 in the angiogenesis of breast cancers. Cancer cell international. 2015;15(1):17.

33. Lacal PM, Graziani G. Therapeutic implication of vascular endothelial growth factor receptor-1 (VEGFR-1) targeting in cancer cells and tumor microenvironment by competitive and non-competitive inhibitors. Pharmacological research. 2018;136:97–107.
34. Fedele M, Cerchia L, Chiappetta G. The Epithelial-to-Mesenchymal Transition in Breast Cancer: Focus on Basal-Like Carcinomas. Cancers. 2017;9(10).
35. Zhang H, Song Y, Yang H, Liu Z, Gao L, Liang X, et al. Tumor cell-intrinsic Tim-3 promotes liver cancer via NF-kappaB/IL-6/STAT3 axis. Oncogene. 2018;37(18):2456–68.
36. Barbi J, Pardoll D, Pan F. Treg functional stability and its responsiveness to the microenvironment. Immunological reviews. 2014;259(1):115–39.
37. Mu X, Shi W, Xu Y, Xu C, Zhao T, Geng B, et al. Tumor-derived lactate induces M2 macrophage polarization via the activation of the ERK/STAT3 signaling pathway in breast cancer. Cell cycle. 2018;17(4):428–38.
38. Muendlein HI, Sarhan J, Liu BC, Connolly WM, Schworer SA, Smirnova I, et al. Constitutive Interferon Attenuates RIPK1/3-Mediated Cytokine Translation. Cell reports. 2020;30(3):699–713 e4.
39. Najafi M, Hashemi Goradel N, Farhood B, Salehi E, Nashtaei MS, Khanlarkhani N, et al. Macrophage polarity in cancer: A review. Journal of cellular biochemistry. 2019;120(3):2756–65.
40. Gordon S, Martinez FO. Alternative activation of macrophages: mechanism and functions. Immunity. 2010;32(5):593–604.
41. Varin A, Gordon S. Alternative activation of macrophages: immune function and cellular biology. Immunobiology. 2009;214(7):630–41.
42. Balce DR, Li B, Allan ER, Rybicka JM, Krohn RM, Yates RM. Alternative activation of macrophages by IL-4 enhances the proteolytic capacity of their phagosomes through synergistic mechanisms. Blood. 2011;118(15):4199–208.
43. Song G, Ouyang G, Bao S. The activation of Akt/PKB signaling pathway and cell survival. Journal of cellular and molecular medicine. 2005;9(1):59–71.
44. Vergadi E, Ieronymaki E, Lyroni K, Vaporidi K, Tsatsanis C. Akt Signaling Pathway in Macrophage Activation and M1/M2 Polarization. Journal of immunology. 2017;198(3):1006–14.

Supplementary Materials

Figure S1: Correlation between eIF4E and prognosis of various types of cancer Correlation between eIF4E and prognosis of various types of cancer in the GEPIA, Table S1: Geo database data set GSE109169 differentially expressed genes. Table S2: eIF4E co expressed differential genes. Table S3: eIF4E co-expression gene GO_BP enrichment analysis. Table S4: Enrichment analysis of eIF4E co-expression gene KEGG. Table S5: eIF4E co-expression of PPI network in breast. Table S6: eIF4E co-expression TF-miRNA network.

Figures

FIGURE 1

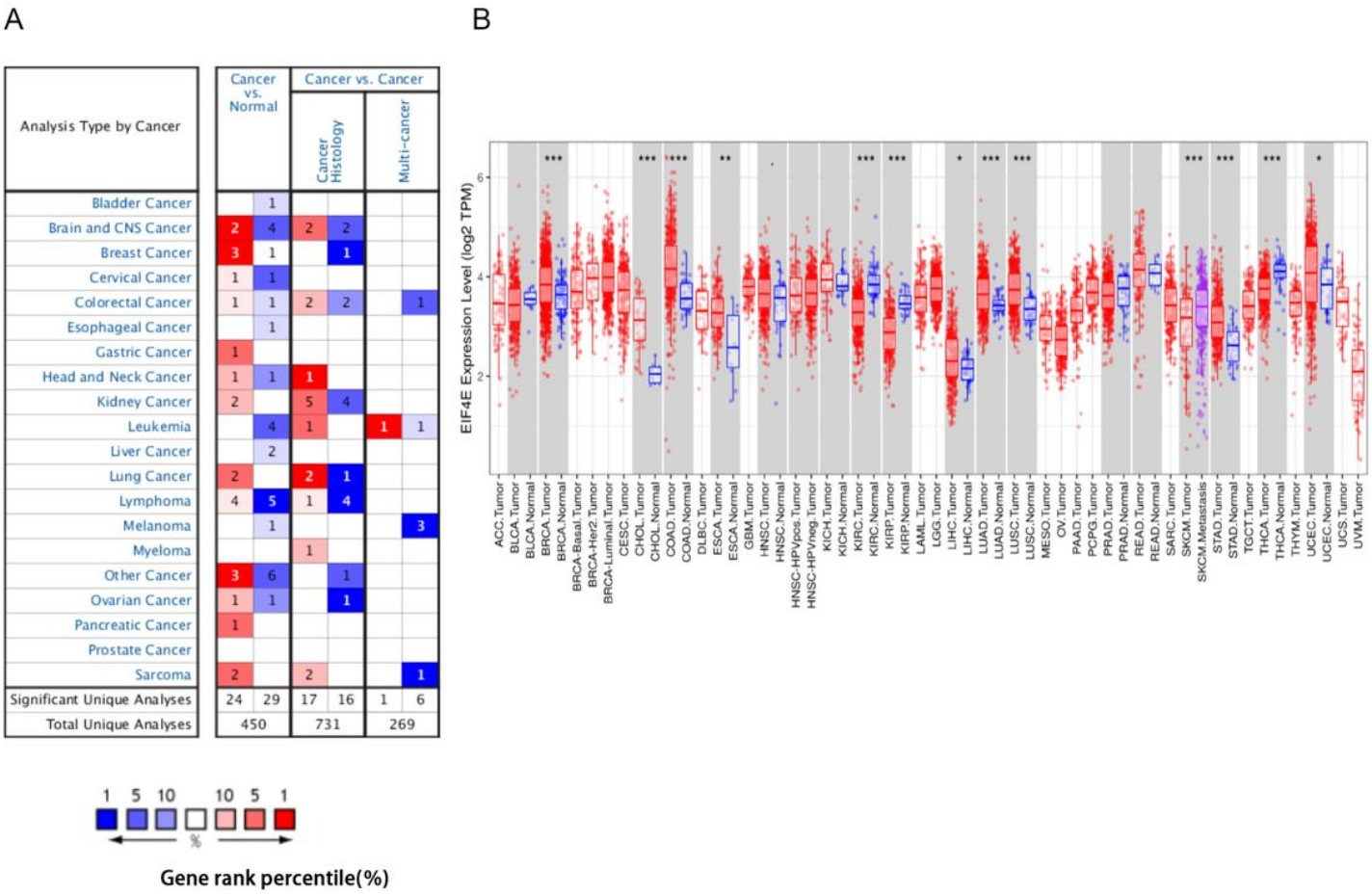

Figure 1

The expression level of eIF4E in different types of tumor tissues and normal tissues (A) The expression level of eIF4E in different types of tumor tissues and normal tissues in the Oncomine database. (P value is .001, fold change is 1.5, and gene ranking of all.) (B) The expression level of eIF4E in different types of tumor tissues and normal tissues in TIMER database (*, $p < 0.05$; **, $p < 0.01$; ***, $p < 0.001$)

FIGURE 2

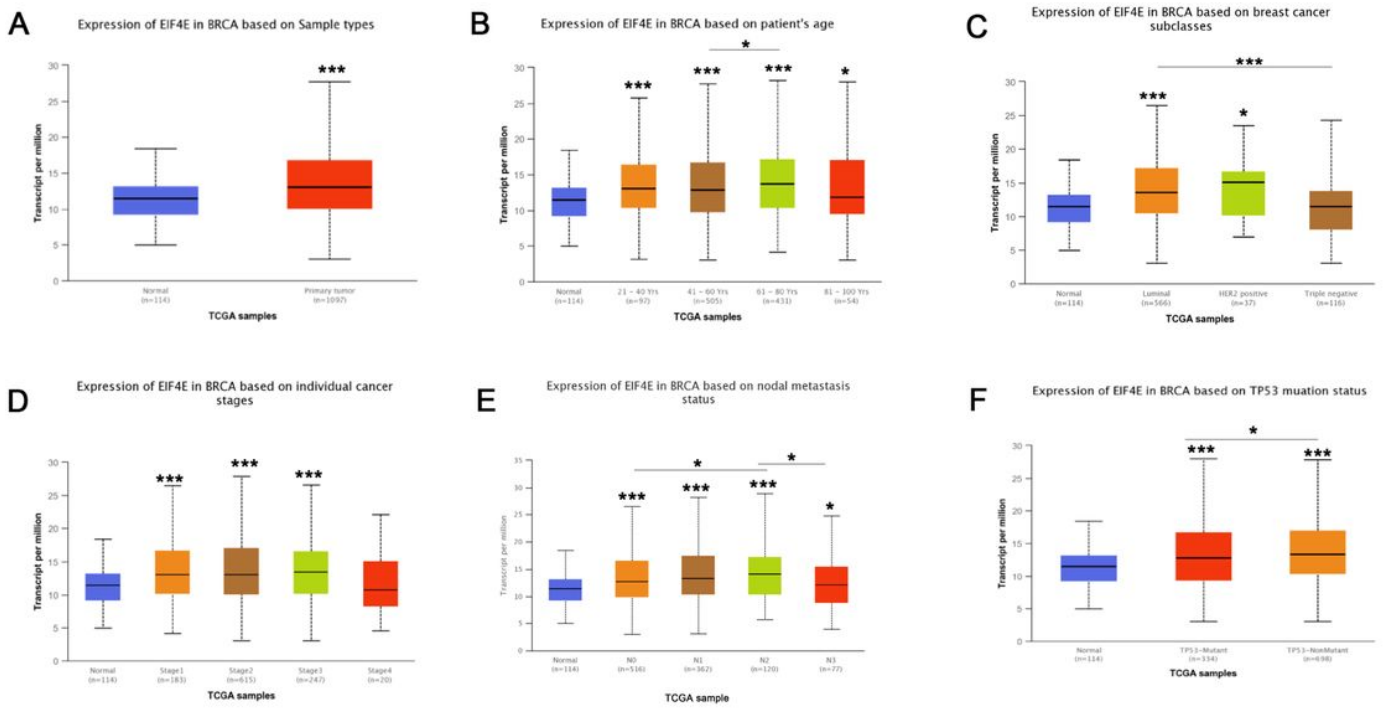

Figure 2

eIF4E transcription in subgroups of patients with BRCA, stratified based on gender, age and other criteria (UALCAN). Box-whisker plots showing the expression of eIF4E in sub groups of BRCA samples. (A) Boxplot showing relative expression of eIF4E in normal and BRCA samples. (B) Boxplot showing relative expression of eIF4E in normal individuals of any age or in BRCA patients aged 21-40, 41-60, 61-80, or 81-100 yr. (C) Boxplot showing relative expression of eIF4E in BRCA based on breast cancer subclasses. (D) Boxplot showing relative expression of eIF4E in normal individuals or in BRCA patients in stages 1, 2, 3 or 4. (E)Boxplot showing relative expression of eIF4E in BRCA based on nodal metastasis status. (F) Boxplot showing relative expression of eIF4E in BRCA based on TP53 mutation status.The central mark is the median; the edges of the box are the 25th and 75th percentiles. The t-test was used to estimate the significance of difference in gene expression levels between groups. *, $p < 0.05$; **, $p < 0.01$; ***, $p < 0.001$.

FIGURE 3

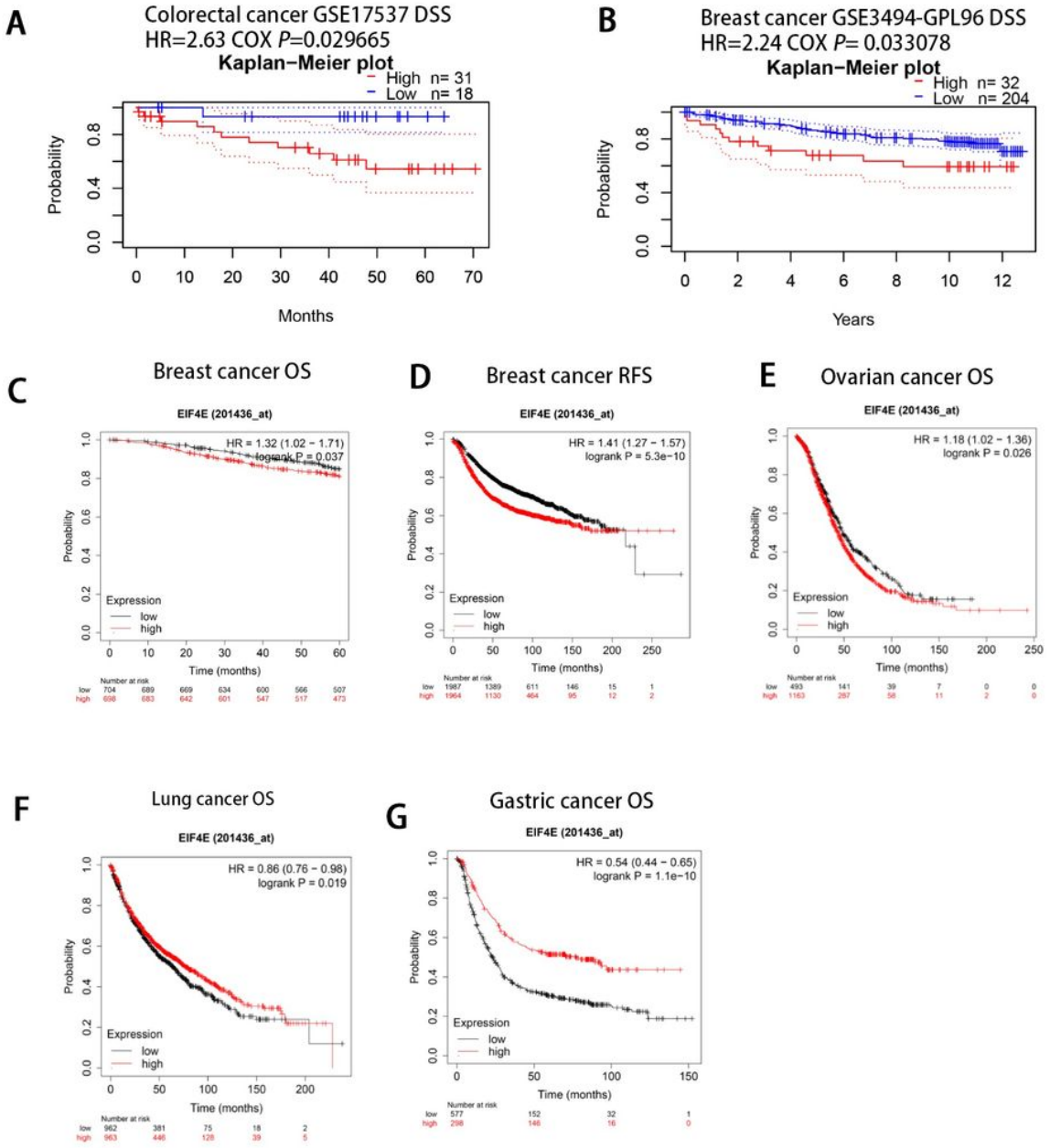

Figure 3

Correlation between eIF4E and prognosis of various types of cancer Correlation between eIF4E and prognosis of various types of cancer in the PrognoScan (A–B) Correlation between eIF4E and prognosis of various types of cancer in the Kaplan-Meier plotter database (C–G). OS, overall survival; DSS,disease free survival; RFS, recurrence-free survival

FIGURE 4

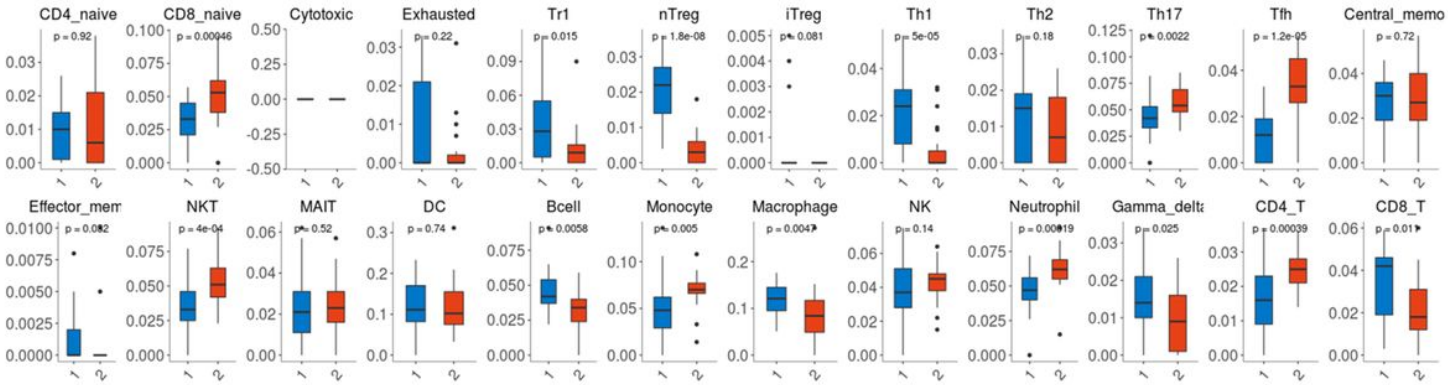

Figure 4

Immune cell abundance analysis between the breast cancer tumor tissues and adjacent normal tissues in GSE109169 to estimate the abundance of immune cell infiltration. *, $p < 0.05$; **, $p < 0.01$; ***, $p < 0.001$. (blue box: breast cancer group; red box: normal group)

FIGURE 5

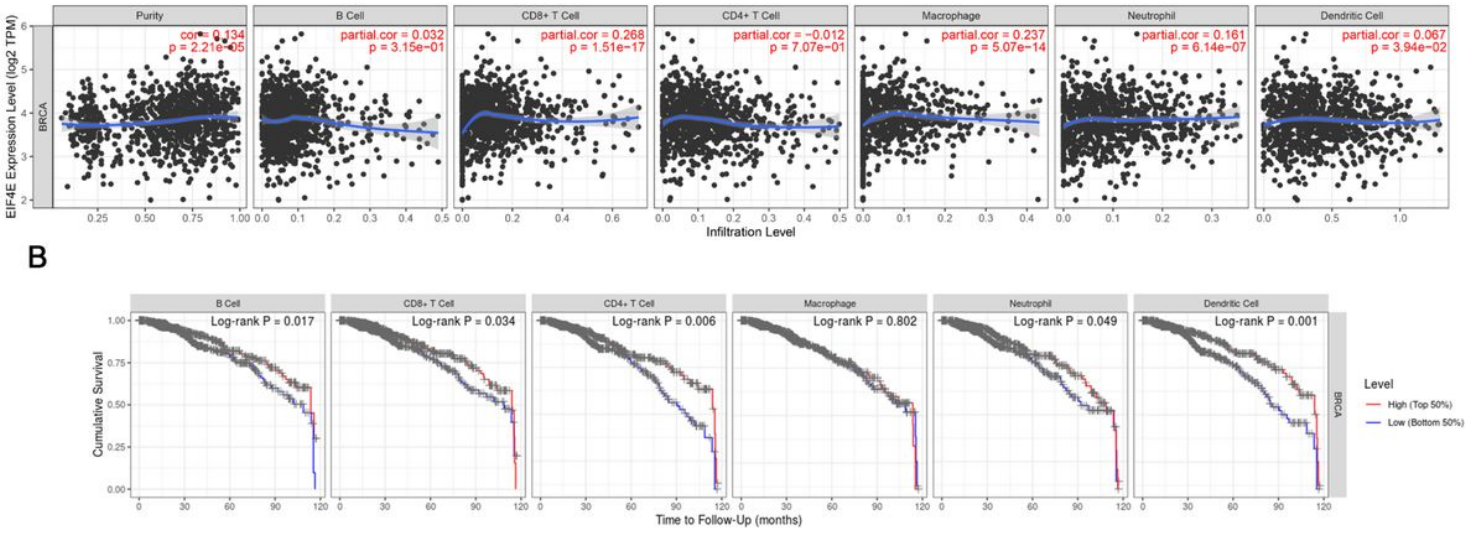

	B_cell	CD8_Tcell	CD4_Tcell	Macrophage	Neutrophil	Dendritic	EIF4E
lower limit	0.005	0.032	0.049	0.589	0.013	0.088	1.085
hazard ratio	0.272	0.329	1.896	7.037	1.846	0.619	1.482
upper limit	16.268	3.420	73.425	84.123	259.922	4.385	2.025

Figure 5

eIF4E expression is correlated with the level of immune infiltration in BRCA. (A) eIF4E expression is correlated with the level of immune infiltration in BRCA. (B) Kaplan-Meier plots of immune infiltration in BRCA. (C) Multivariable hazards models were used to evaluate the impacts of eIF4E expression on survival in the presence of infiltrating levels of multiple immune cells. *, $p < 0.05$; **, $p < 0.01$; ***, $p < 0.001$.

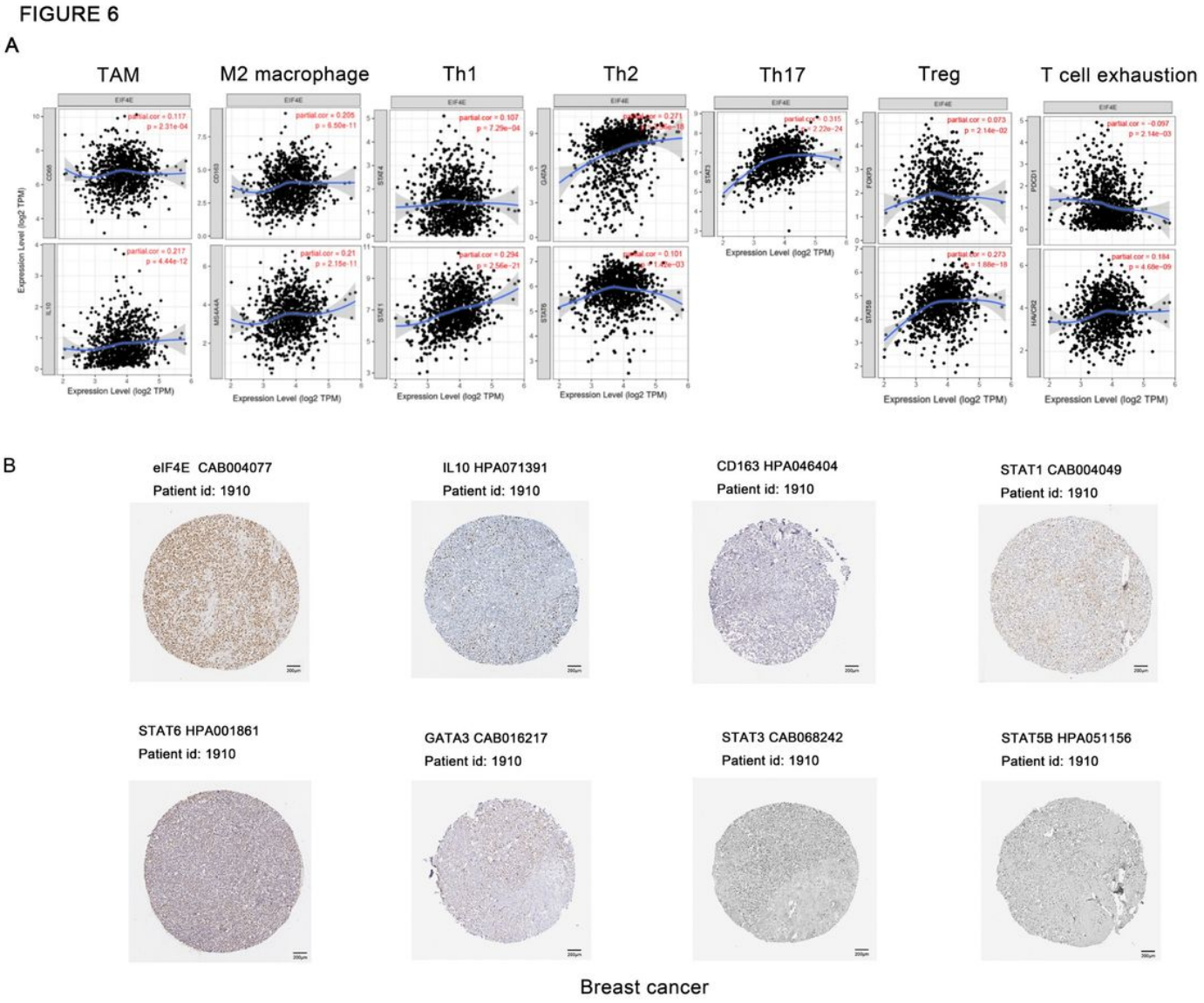

Figure 6

Correlation analysis between eIF4E and immune marker expression. (A) Scatterplots of correlations between eIF4E expression and gene markers of TAMs, M2 macrophages and Th1 and Th2 and Th17 and Treg and T cell exhaustion in BRCA. (B)Immunohistochemical map of HPA database showing significant expression levels of eIF4E related immune cell markers(Scale bar,200μm).

FIGURE 7

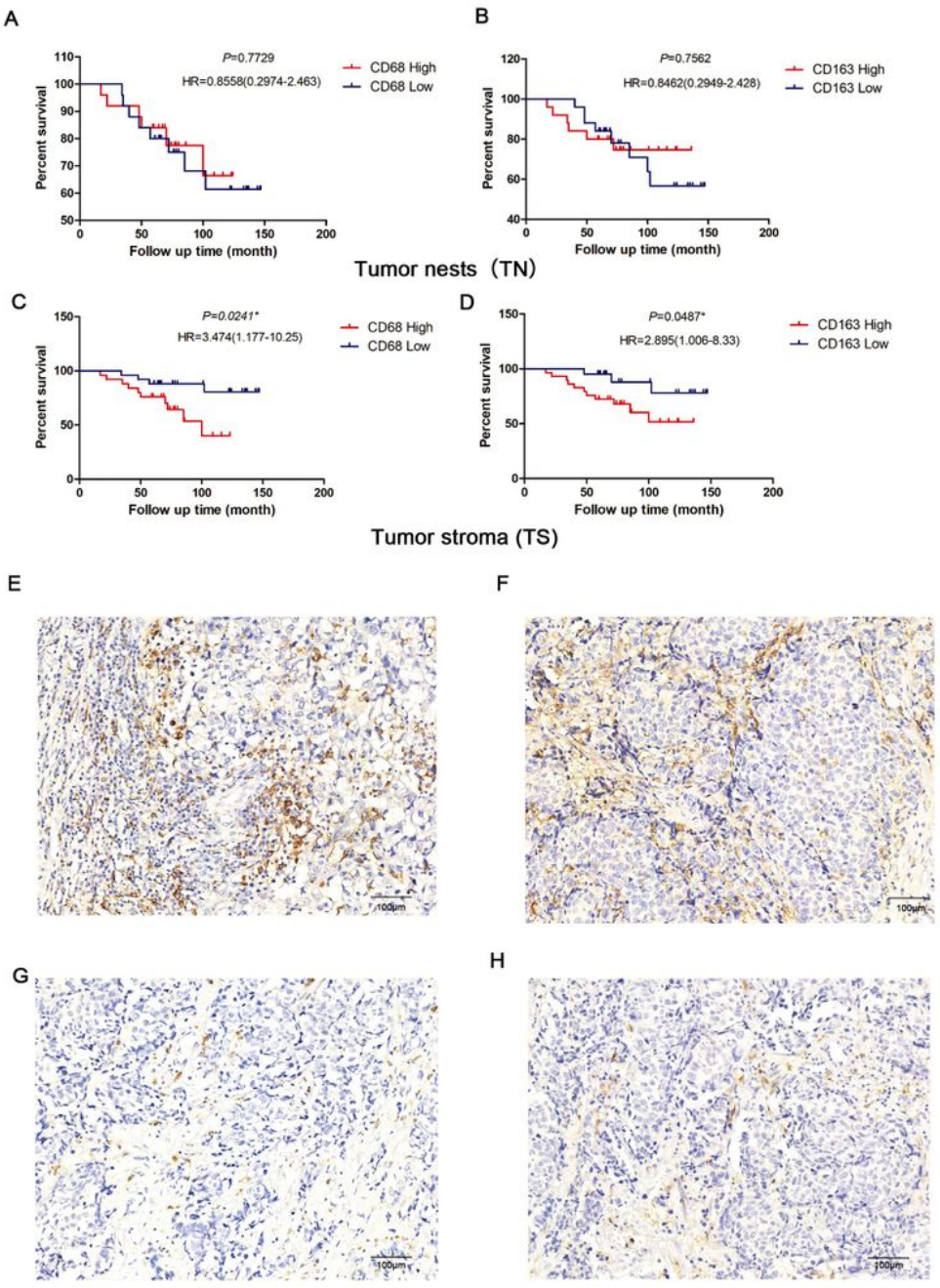

Figure 7

OS curves based on macrophage properties and the density and distribution pattern of macrophage infiltration characterized by CD68+ and CD163+ immunoreactivity in the tumor nest (TN) and tumor stroma (TS). A–D Overall survival curves by CD68+ positive macrophage infiltration into the tumor nest (A) and stroma (C). Overall survival curves by CD163+ positive M2 macrophage infiltration into the tumor nest (B) and stroma (D). Representative images of high density of CD68+ staining (E) and CD163+

staining (F) in TN and TS. Representative images of low density of CD68+ staining (G)and CD163 staining (H) in TN and TS. Scale bar, 100 μm

FIGURE 8

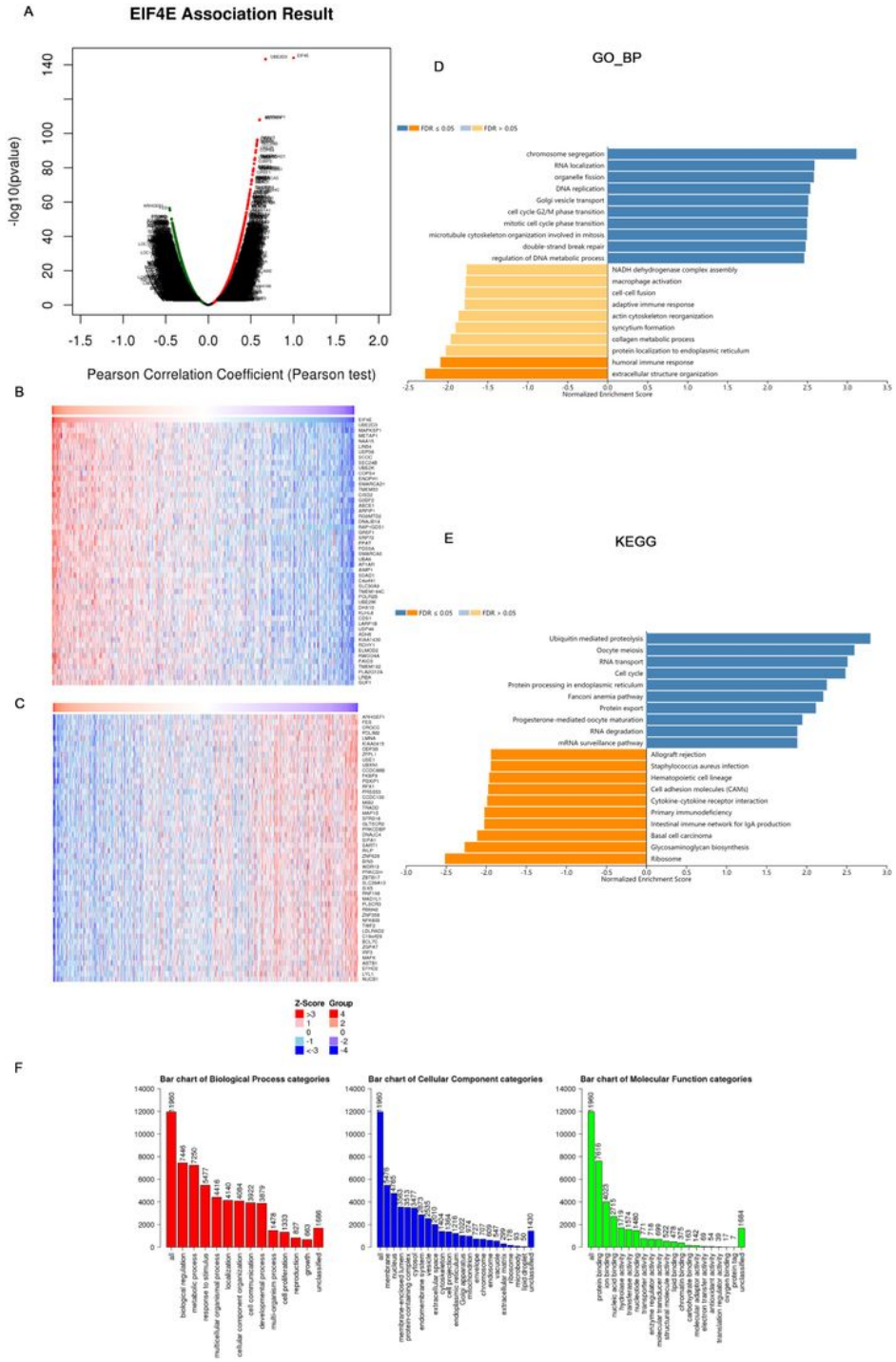

Figure 8

eIF4E co-expression genes in BRCA (LinkedOmics). (A) The global eIF4E highly correlated genes identified by Pearson test in BRCA cohort. (B-C) Heat maps showing top 50 genes positively and negatively correlated with eIF4E in BRCA. Red indicates positively correlated genes and blue indicates negatively

correlated genes. (D-E) Significantly enriched GO annotations and KEGG pathways of eIF4E in BRCA cohort. (F)Bar chart of Biological process categories, Cellular component categories and Molecular function categories.

FIGURE 9

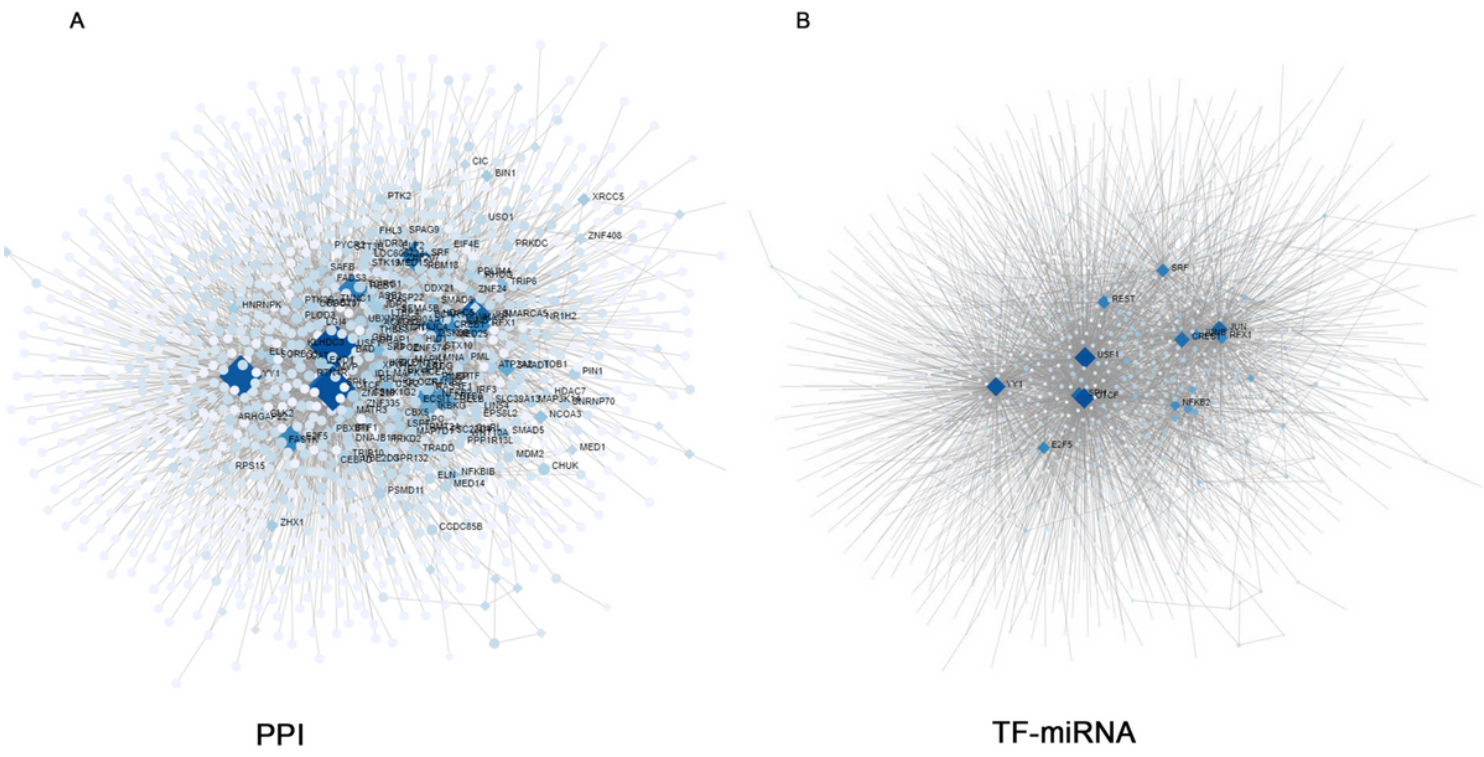

Figure 9

Protein-protein interaction (PPI) and Transcription factor-miRNA (TF-miRNA) regulatory network of eIF4E co-expressed genes (A) The breast-specific PPI network of significantly eIF4E co-expression genes. (B)TF-miRNA coregulatory network of significantly eIF4E co-expression genes.

FIGURE 10

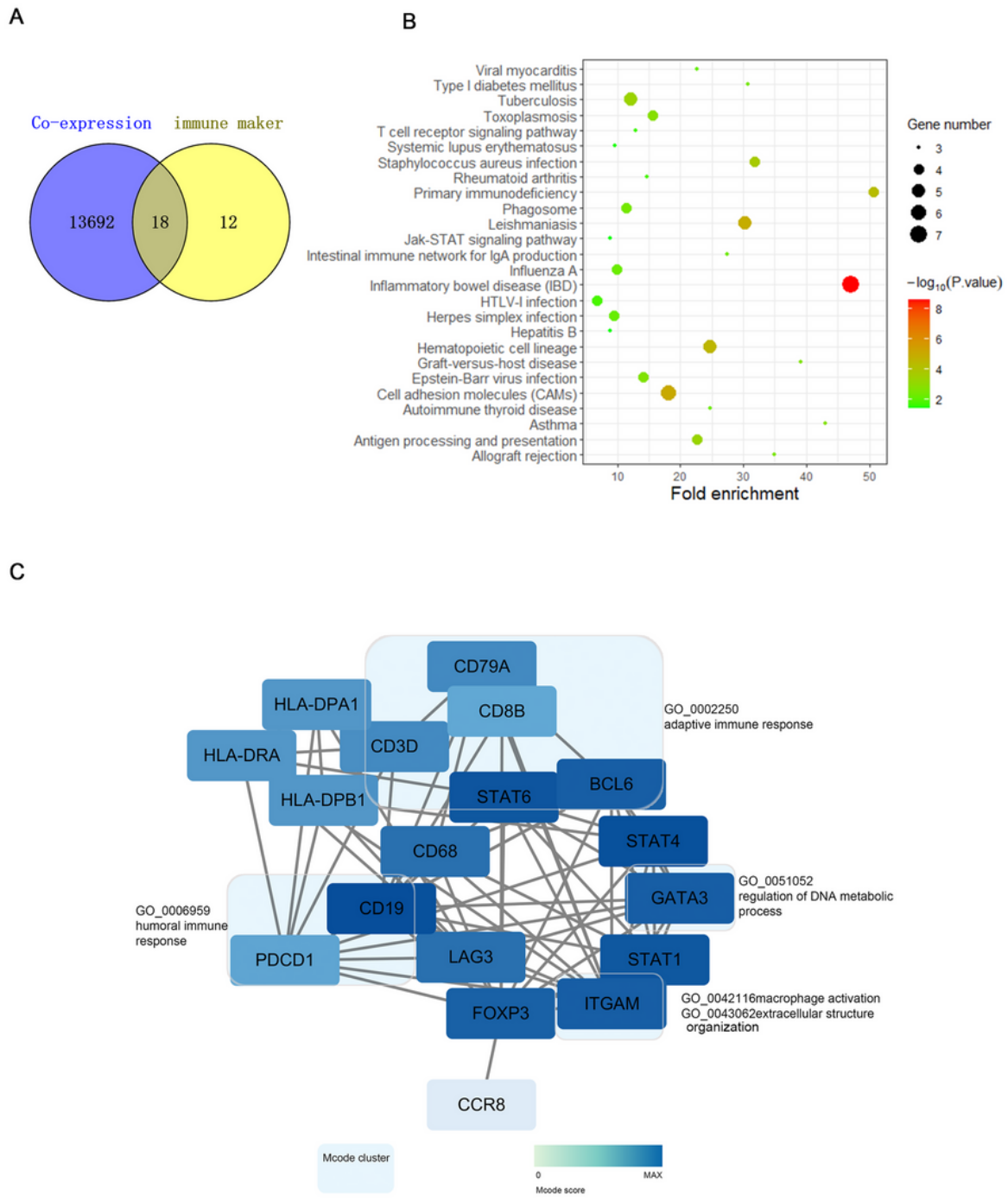

Figure 10

Cross analysis of eIF4E co-expressed genes and immune marker genes. (A) The Venn diagram showing that the eIF4E co-expressed gene overlapped with the immune marker gene. (B) KEGG analysis of genes described in (A). (C) Cytoscape and GO analysis of genes described in (A).

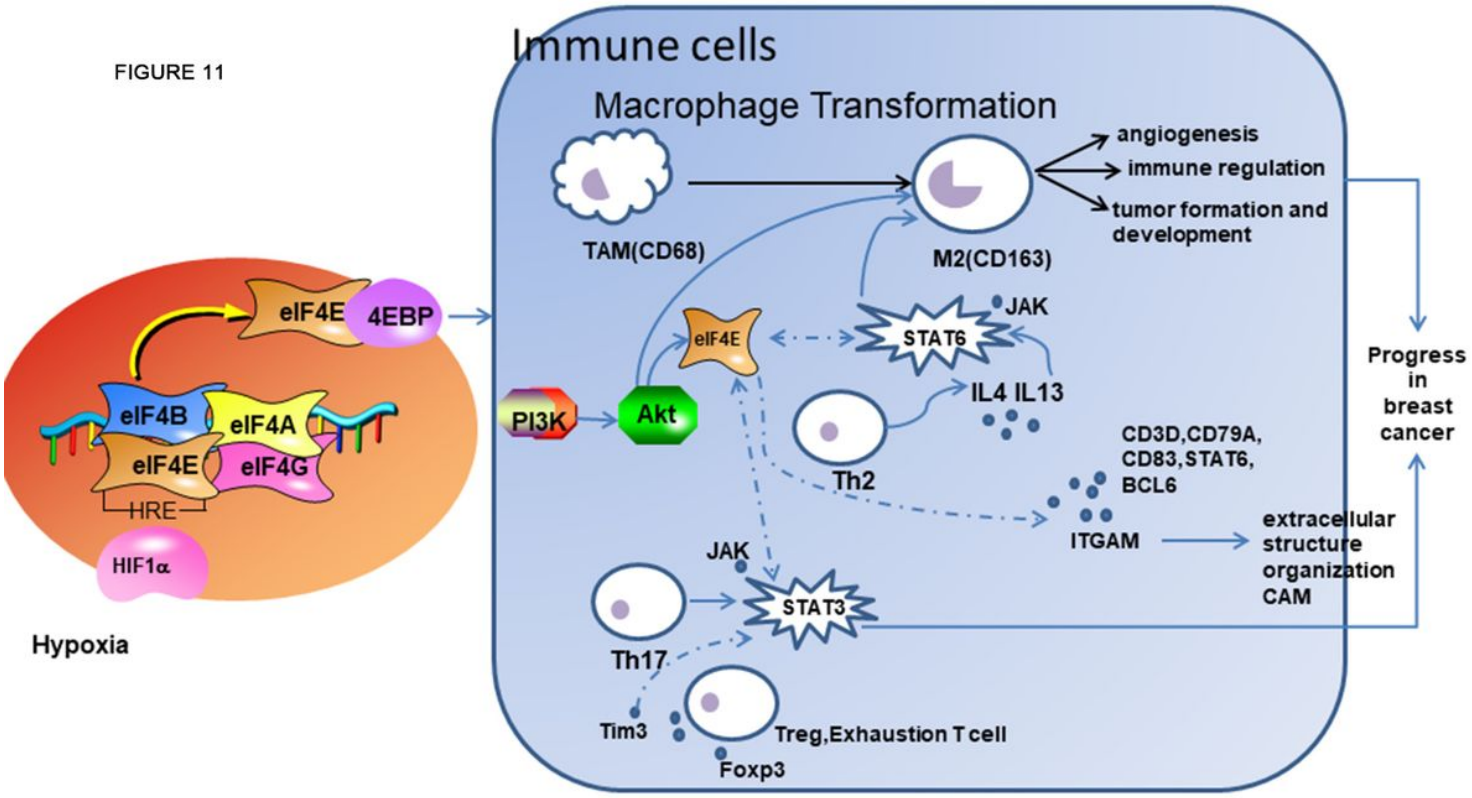

Figure 11

Mechanism of eIF4E regulating immune cell infiltration in breast cancer.

Supplementary Files

This is a list of supplementary files associated with this preprint. Click to download.

- GEPIAS1.tif
- Supplementarytable1.xlsx
- Supplementarytable2.xlsx
- Supplementarytable3.xlsx
- Supplementarytable4.xlsx
- Supplementarytable5.xlsx
- Supplementarytable6.xlsx